Effect of Holstein phonons on the electronic properties of graphene

2008 J. Phys.: Condens. Matter 20 055002

(http://iopscience.iop.org/0953-8984/20/5/055002)

J. Phys.: Condens. Matter **20** (2008) 055002 (7pp) doi:10.1088/0953-8984/20/5/055002

Effect of Holstein phonons on the electronic properties of graphene

T Stauber[1,2] **and N M R Peres**[2]

[1] Instituto de Ciencia de Materiales de Madrid, CSIC, Cantoblanco, E-28049 Madrid, Spain
[2] Center of Physics and Department of Physics, University of Minho, P-4710-057, Braga, Portugal

Received 24 October 2007, in final form 21 December 2007
Published 17 January 2008
Online at stacks.iop.org/JPhysCM/20/055002

Abstract
We obtain the self-energy of the electronic propagator due to the presence of Holstein polarons within the first Born approximation. This leads to a renormalization of the Fermi velocity of 1%. We further compute the optical conductivity of the system at the Dirac point and at finite doping within the Kubo formula. We argue that the effects due to Holstein phonons are negligible and that the Boltzmann approach, which does not include inter-band transitions and can thus not treat optical phonons due to their high energy of $\hbar\omega_0 \sim 0.1$–0.2 eV, remains valid.

(Some figures in this article are in colour only in the electronic version)

1. Introduction

Three years ago, Geim, Novoselov and co-workers succeeded in isolating and contacting a single layer of graphite (graphene) [1]. Contrary to common wisdom, this experiment showed that true two-dimensional lattices are thermodynamically stable [2, 3]. This stability comes about because the system gently crumples to the third direction, forming ripples [4]. It is therefore an important problem to study the effect of out-of-plane phonons on the electronic properties of the system. In contrast to two-dimensional electron systems in semiconductor heterostructures, where (scalar) electrons interact with bulk [5] or surface [6] phonons, in graphene there are two-dimensional in-plane as well as out-of-plane vibrational modes to which Dirac (spinor) fermions will couple.

There are two different vertex types modeling the interaction of electrons with optical phonons. First, due to the atomic displacement within the plane, the tunneling matrix element between two carbon atoms varies. This gives rise to a Su–Schrieffer–Heeger-type coupling (current–current coupling) [7]. The two-dimensional gage field is composed of longitudinal optical (LO) and transverse optical (TO) phonons, which are degenerate at $q = 0$. This vertex type is also found from symmetry arguments [8]. There are also out-of-plane vibrations. These lattice displacements are symmetric with respect to their neighboring atoms and thus couple to the electronic densities. The optical (ZO) modes can then be described within the Holstein model [9]. For a recent account on the Green's function of the Holstein polaron, see [10] and references therein.

Out-of-plane modes are energetically smaller than in-plane vibrations due to the hybridization of the sp^2-orbitals within the graphene sheet. A tight-binding calculation including nearest and second-nearest neighbors yields $\omega_{ZO} \approx \omega_{LO}/2$ for the optical branch close to the Γ-point [11]. For a first-principle calculation of the phonon spectra, see the work by Wirtz and Rubio [12]. The effect of the electron–phonon coupling on the local density of states of zig-zag graphene ribbons has been studied by Sasaki *et al* [13]. The effect of the optical phonons on the Raman spectrum of disordered graphene was studied by Castro Neto and Guinea [14].

The effect of Holstein phonons on transport properties has been receiving renewed interest in the context of the one-dimensional Holstein–Hubbard model [15]. Here, we will discuss Holstein phonons in graphene for the following reason. It is currently believed that transport properties can be described well within a semi-classical Boltzmann approach [16–18]. This implies well-defined quasi-particles, i.e. only one band is considered and inter-band transitions are ruled out. Doing so, several scattering mechanisms have been discussed, ranging from local defects (vacancies or substitutions), long-ranged Coulomb impurities in the substrate or due to adsorbed atoms to acoustical phonons [19, 20].

Optical phonons cannot be treated within the one-band Boltzmann approach[3] since they would induce inter-band transitions at typical densities of $n \lesssim 5 \times 10^{12}$ cm^{-2}. It

[3] For a two-band formulation of the Boltzmann equation, see [21].

is therefore crucial to assess this scattering mechanism via the Kubo formalism. In section 2, we present our model for Holstein phonons and calculate the electronic self-energy within the first Born approximation in section 3. We further compute the optical conductivity in section 4, using the full Green's function, but neglecting vertex corrections. We close with conclusions and outlook.

2. The effective model

In two-dimensional graphene sheets, first-principle calculations reveal that the Born–Oppenheimer approximation is not valid for doped graphene sheets [22]. Fröhlich polarons [23] are thus not a good starting point to describe electron–lattice interaction in graphene. Here, we present a study of the electron–lattice coupling due to localized Holstein phonons in a two-dimensional honeycomb lattice, thus treating the ZO phonons (out-of-plane vibrations).

The honeycomb lattice (the lattice of graphene) is made of two interpenetrating triangular lattices, defining two non-equivalent sites, usually labeled as A and B sites [24]. The model Hamiltonian for ZO polarons in graphene reads as follows:

$$H - t\sum_{i,\sigma\delta}\left[a^\dagger_\sigma(\boldsymbol{R}_i)b_\sigma(\boldsymbol{R}_i+\boldsymbol{\delta})+\text{H.c.}\right]+\sum_q \omega_q c^\dagger_q c_q + V_{\text{ep}} \quad (1)$$

where $a^\dagger_\sigma(\boldsymbol{R}_i)$ ($b^\dagger_\sigma(\boldsymbol{R}_i)$) creates an electron at an atom of the A (B) sub-lattice and $c^\dagger_q$ are creation phonon operators. The energy ω_q is the dispersion of the ZO phonon and V_{ep} is the electron–phonon interaction. We model the coupling to the ZO phonons as the usual density–density coupling [25]

$$V_{\text{ep}} = D\sum_{\sigma,i,j}\left[a^\dagger_\sigma(\boldsymbol{R}_i)a_\sigma(\boldsymbol{R}_i)+b^\dagger_\sigma(\boldsymbol{R}_i)b_\sigma(\boldsymbol{R}_i)-1\right]Q_j, \quad (2)$$

with Q_j defined as

$$Q_j = \sum_q X_q \mathrm{e}^{\mathrm{i}q\cdot\boldsymbol{R}_j}(c_q + c^\dagger_{-q}), \quad (3)$$

and

$$X_q = \sqrt{\frac{\hbar^2}{2MN\omega_q}} \quad (4)$$

and M is the ion's mass and N is the number of unit cells in the crystal. Note that we couple the density with respect to the half-filled band such that particle–hole symmetry is conserved by reversing the sign of the coupling constant. In the following, though, we shall neglect this shift in the bosonic operators.

The effect of Holstein polarons is obtained using $\omega_q \simeq \omega_0$ and transforming the operators in Hamiltonian (1) to momentum space. This gives

$$H = -t\sum_{q,\sigma}\left(\phi_q a^\dagger_{q,\sigma}b_{q,\sigma}+\text{H.c.}\right)+\sum_q \omega_0 c^\dagger_q c_q + V_{\text{ep}}, \quad (5)$$

with $\phi_q = \sum_\delta \mathrm{e}^{-\mathrm{i}\delta\cdot q}$, δ being the vectors connecting the three nearest neighbors on the honeycomb lattice, and V_{ep} being given by

$$V_{\text{ep}} = D\sum_{p,q,\sigma} X_q\left(a^\dagger_{p,\sigma}a_{p+q,\sigma}+b^\dagger_{p,\sigma}b_{p+q,\sigma}\right)(c_q + c^\dagger_{-q}). \quad (6)$$

Let us comment on the coupling constant D. Due to the mirror symmetry of the graphene sheet, one might think that the linear coupling to lattice displacements is zero. But the mirror symmetry is broken for samples where graphene lies on top of a SiO_2 or SiC substrate (for a discussion, see [8]). To quantify the coupling constant in terms of the dimensionless constant $g = \sqrt{N}DX_0/\omega_0$, we assume that the coupling mechanism is due to a variation of the hopping matrix element. This yields g of the order of unity [14].

3. Second-order perturbation theory

If the phonon energy scale is much smaller than the electronic energy scale, Migdal's theorem states that it is sufficient to calculate the lowest-order self-energy diagram [26]. This diagram can further be calculated using the bare electron Green's function. Still, the importance of electron–phonon coupling also depends on the dimensionality of the system. For example, in self-assembled quantum dots, vertex 'corrections' to the polarization of an electron–hole pair give rise to charge cancellation [27], thus changing the optical conductivity significantly [28]. Also, for A_3C_{60} (A = K, Rb) [29] and for general one-dimensional systems, [30] Migdal's theorem is not valid. Furthermore, electron–electron interaction can affect the effective electron–phonon interaction [15].

In graphene sheets, electron–electron interaction is generally neglected, i.e. one assumes a 'normal' ground state at zero doping (one electron per unit cell)—characterized by a semi-metal. Since the average kinetic and interaction energy per particle both scale with $\sqrt{n}$ where n is the carrier density, the interaction does not become important at finite doping either. Electron–electron interaction is also neglected in recent works on localization [31] even though disorder enhances the effect of interaction [32]. The same should hold for the electron–phonon vertex corrections, which results in an effective electron–electron interaction, and we thus believe that the assumption of Migdal's theory is a good starting point to discuss the Holstein phonons in graphene.

Because of the existence of two sub-lattices, the Green's function needs to be written as a 2×2 matrix:

$$\boldsymbol{G}_\sigma(\boldsymbol{k},\tau) = \begin{pmatrix} G_{\text{AA},\sigma}(\boldsymbol{k},\tau) & G_{\text{AB},\sigma}(\boldsymbol{k},\tau) \\ G_{\text{BA},\sigma}(\boldsymbol{k},\tau) & G_{\text{BB},\sigma}(\boldsymbol{k},\tau)\end{pmatrix} \quad (7)$$

with

$$\begin{aligned} G_{\text{AA},\sigma}(\boldsymbol{k},\tau) &= -\langle\mathcal{T}a_{k,\sigma}(\tau)a^\dagger_{k,\sigma}(0)\rangle, \\ G_{\text{AB},\sigma}(\boldsymbol{k},\tau) &= -\langle\mathcal{T}a_{k,\sigma}(\tau)b^\dagger_{k,\sigma}(0)\rangle, \\ G_{\text{BA},\sigma}(\boldsymbol{k},\tau) &= -\langle\mathcal{T}b_{k,\sigma}(\tau)a^\dagger_{k,\sigma}(0)\rangle, \\ G_{\text{BB},\sigma}(\boldsymbol{k},\tau) &= -\langle\mathcal{T}b_{k,\sigma}(\tau)b^\dagger_{k,\sigma}(0)\rangle, \end{aligned} \quad (8)$$

where τ is the 'imaginary' time, and $\mathcal{T}$ is the time ordering operator.

Up to second order in perturbation theory, and after transforming the time dependence of the Green's function to Matsubara frequencies, we obtain the following result:

$$\boldsymbol{G} = \boldsymbol{G}^{(0)} + \boldsymbol{G}^{(0)}\boldsymbol{\Sigma}\boldsymbol{G}^{(0)}, \quad (9)$$

where the matrix $\boldsymbol{\Sigma}$ is defined as

$$\boldsymbol{\Sigma} = \begin{pmatrix} \Sigma_{AA} & \Sigma_{AB} \\ \Sigma_{BA} & \Sigma_{BB} \end{pmatrix}, \tag{10}$$

and the matrix element $\Sigma_{\alpha\beta}$ is defined by ($\alpha, \beta = A, B$)

$$\Sigma_{\alpha\beta}(i\omega_n, \boldsymbol{p}) = -\frac{1}{\beta}\sum_{\boldsymbol{q},\nu} D^2 X_{\boldsymbol{q}}^2 D^{(0)}(\boldsymbol{q}, i\nu) \times G^{(0)}_{\alpha\beta}(\boldsymbol{p}-\boldsymbol{q}, i\omega_n - i\nu). \tag{11}$$

Because both $X_{\boldsymbol{q}}$ and $D^{(0)}(\boldsymbol{q}, i\nu)$ are momentum independent, i.e. we set $\omega_{\boldsymbol{q}} = \omega_0$ and the phonon propagator $D^{(0)}(\boldsymbol{q}, i\nu)$ is given by

$$D^{(0)}(\boldsymbol{q}, i\nu) = \frac{2\omega_0}{(i\nu)^2 - \omega_0^2}, \tag{12}$$

the matrix elements of the self-energy matrix can be written in a simplified form, reading $\Sigma_{\alpha\beta}(i\omega_n) = -\frac{1}{\beta}\sum_{\boldsymbol{q},\nu} D^2 X_0^2 D^{(0)}(i\nu) G^{(0)}_{\alpha\beta}(\boldsymbol{q}, i\omega_n + i\nu)$, where X_0 is $X_{\boldsymbol{q}}$ with $\omega_{\boldsymbol{q}}$ replaced by ω_0. Notice that we neglected the constant shift in the self-energy due to the shift of the bosonic displacement operator, still present in equation (11). This is consistent, since we also neglected the Hartree correction to the self-energy.

From the above we can write down a Dyson equation for the electronic propagator, given by

$$\boldsymbol{G} = \boldsymbol{G}^{(0)} + \boldsymbol{G}^{(0)}\boldsymbol{\Sigma}\boldsymbol{G}, \tag{13}$$

which has to be solved for $\boldsymbol{G}$. The equation giving the Matsubara Green's function for the free electronic system reads

$$\begin{pmatrix} i\omega_n & -t\phi(\boldsymbol{k}) \\ -t\phi^*(\boldsymbol{k}) & i\omega_n \end{pmatrix} \boldsymbol{G}^{(0)}(i\omega_n, \boldsymbol{k}) = \mathbf{1}, \tag{14}$$

and $\mathbf{1}$ is the 2×2 unit matrix. Within the Dirac cone approximation, which applies in a range of 1 eV, one has $\Sigma_{AB}(i\omega_n) = \Sigma_{BA}(i\omega_n) = 0$. Also, the following result holds, $\Sigma_{AA}(i\omega_n) = \Sigma_{BB}(i\omega_n) = \Sigma(i\omega_n)$, leading to a simplified form for the Dyson equation (13), which can be readily solved, giving

$$\boldsymbol{G} = \frac{\begin{pmatrix} i\omega_n - \Sigma(i\omega_n) & t\phi(\boldsymbol{k}) \\ t\phi^*(\boldsymbol{k}) & i\omega_n - \Sigma(i\omega_n) \end{pmatrix}}{(i\omega_n - \Sigma)(i\omega_n - \Sigma) - t^2|\phi|^2}. \tag{15}$$

The matrix elements of equation (15) can be put into a simpler form reading

$$G_{AA}(\omega_n, \boldsymbol{k}) = \sum_{j=\pm1} \frac{1/2}{i\omega_n - \Sigma(i\omega_n) - jt|\phi(\boldsymbol{k})|}, \tag{16}$$

$$G_{AB}(\omega_n, \boldsymbol{k}) = \sum_{j=\pm1} \frac{je^{i\delta(\boldsymbol{k})}/2}{i\omega_n - \Sigma(i\omega_n) - jt|\phi(\boldsymbol{k})|}, \tag{17}$$

$$G_{BA}(\omega_n, \boldsymbol{k}) = \sum_{j=\pm1} \frac{je^{-i\delta(\boldsymbol{k})}/2}{i\omega_n - \Sigma(i\omega_n) - jt|\phi(\boldsymbol{k})|}, \tag{18}$$

$$G_{BB}(\omega_n, \boldsymbol{k}) = G_{AA}(\omega_n, \boldsymbol{k}). \tag{19}$$

The summation over the bosonic frequency ν in equation (3) can be performed using standard methods, leading to

$$\Sigma(i\omega_n) = \sum_{\boldsymbol{q}, j=\pm1} D^2 X_0^2 \frac{1}{2}\left(\frac{N_0 + n_F(jt|\phi(\boldsymbol{q})|)}{i\omega_n - jt|\phi(\boldsymbol{q})| + \omega_0} + \frac{N_0 + 1 - n_F(jt|\phi(\boldsymbol{q})|)}{i\omega_n - jt|\phi(\boldsymbol{q})| - \omega_0}\right). \tag{20}$$

The integrals over the momentum variable in equation (20) can be computed easily at zero temperature and within the Dirac cone approximation, yielding an explicit form for the self-energy.

3.1. Zero doping

At zero temperature and zero chemical potential (that is, at the neutrality point) the self-energy, denoted by $\Sigma \to \Sigma_0$, has a simplified form reading

$$\Sigma_0(i\omega_n) = \frac{g^2\omega_0^2}{N\hbar^2}\sum_{\boldsymbol{q}} \frac{1}{2}\left(\frac{1}{i\omega_n - t|\phi(\boldsymbol{q})|/\hbar - \omega_0/\hbar} + \frac{1}{i\omega_n + t|\phi(\boldsymbol{q})|/\hbar + \omega_0/\hbar}\right) \tag{21}$$

where we have introduced the missing $\hbar$s omitted in the beginning of this section and g denotes a dimensionless coupling constant of order unity, defined below equation (6). Performing the analytical continuation $i\omega_n \to \omega + i\delta$ and computing the momentum integral in equation (21), one obtains the retarded self-energy, $\Sigma^{ret}(\omega)$, of the polaron problem, which reads

$$\Sigma_0^{ret}(\omega) = \frac{A_c}{2\pi}\left(\frac{g\omega_0}{\hbar}\right)^2\left(-\frac{\omega}{v_F^2}\ln\left|\frac{(v_F k_c)^2}{\omega^2 - (\omega_0/\hbar)^2}\right| + \frac{\omega_0/\hbar}{v_F^2}\ln\left|\frac{\omega + \omega_0/\hbar}{\omega - \omega_0/\hbar}\right|\right) - i\pi\frac{A_c}{2\pi}\left(\frac{g\omega_0}{\hbar}\right)^2 \times \left[\left(\frac{\omega}{v_F^2} - \frac{\omega_0}{v_F^2\hbar}\right)\theta(\omega - \omega_0/\hbar)\theta(v_F k_c + \omega_0/\hbar - \omega) - \left(\frac{\omega}{v_F^2} + \frac{\omega_0}{v_F^2\hbar}\right)\theta(-\omega - \omega_0/\hbar)\theta(v_F k_c + \omega_0/\hbar + \omega)\right], \tag{22}$$

with $\pi k_c^2 = (2\pi)^2/A_c$, $A_c = a^2 3\sqrt{3}/2$, and $a = 1.42$ Å.

One can easily obtain the renormalization of the electronic spectrum due to the retarded self-energy induced by the phonons, using Rayleigh–Schrödinger perturbation theory [25]. In this scheme, the ω dependence of the self-energy is replaced by the bare electronic dispersion. Close to the Dirac point, the dispersion is simply given by $\omega = \pm v_F k$, where the upper (lower) sign holds for electrons (holes), and we obtain the new energy spectrum $E(\boldsymbol{k})$ from

$$E(\boldsymbol{k}) = v_F\hbar k + \hbar\,\mathrm{Re}\,\Sigma_0^{ret}(v_F k) \tag{23}$$

for the conduction band and

$$E(\boldsymbol{k}) = -v_F\hbar k + \hbar\,\mathrm{Re}\,\Sigma_0^{ret}(-v_F k) \tag{24}$$

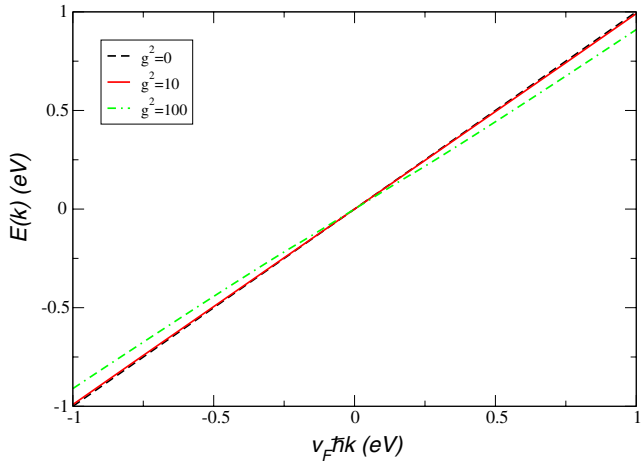

Figure 1. Renormalized energy band at the neutrality point, given by $E(\boldsymbol{k}) = \pm v_{\mathrm{F}}\hbar k \pm \hbar \mathrm{Re}\Sigma_0^{\mathrm{ret}}(v_{\mathrm{F}}k)$ for two different values of the coupling constant g.

for the valence band. Electron–hole symmetry is thus preserved if $\mathrm{Re}\Sigma_0^{\mathrm{ret}}(x) = -\mathrm{Re}\Sigma_0^{\mathrm{ret}}(-x)$, which is the case (see equation (22)).

Considering that $v_{\mathrm{F}}k$ is the smallest energy in the problem, that is, k is very close to the Dirac point, we obtain for $\mathrm{Re}\Sigma_0^{\mathrm{ret}}(v_{\mathrm{F}}k)$ the result

$$\mathrm{Re}\Sigma_0^{\mathrm{ret}}(v_{\mathrm{F}}k) = -v_{\mathrm{F}}k\frac{A_{\mathrm{c}}}{\pi v_{\mathrm{F}}^2}\left(\frac{g\omega_0}{\hbar}\right)^2 \ln\frac{v_{\mathrm{F}}k_c}{\omega_0/\hbar}. \qquad (25)$$

Considering the out-of-plane optical mode of graphene [12], which has an energy of $\omega_{ZO} \simeq 0.1$ eV and using $g^2 = 10$, we obtain

$$\frac{A_{\mathrm{c}}}{\pi v_{\mathrm{F}}^2}\left(\frac{g\omega_0}{\hbar}\right)^2 \ln\frac{v_{\mathrm{F}}k_c}{\omega_0/\hbar} \simeq 0.02. \qquad (26)$$

In figure 1, the renormalized energy dispersion is shown for various values of the coupling constant. We also included a large coupling constant $g = 10$ for better illustration of the effect of the electron–phonon interaction.

3.2. Finite doping

At finite doping, the one-particle dispersion $j|\phi(\boldsymbol{k})|$ must be replaced by $j|\phi(\boldsymbol{k})| - \mu$ in equations (16)–(19) and equation (20), where $\mu = \hbar v_{\mathrm{F}}k_{\mathrm{F}}$ denotes the Fermi energy. The retarded self-energy can then be written as $\Sigma_\mu^{\mathrm{ret}}(\omega) = \Sigma_0^{\mathrm{ret}}(\omega + \mu/\hbar) + \Delta\Sigma(\omega + \mu/\hbar)$, where we have

$$\begin{aligned}\Delta\Sigma(\omega) = {} & \frac{A_{\mathrm{c}}}{2\pi}\left(\frac{g\omega_0}{\hbar}\right)^2 \\ & \times\left(-\frac{\omega_0/\hbar}{v_{\mathrm{F}}^2}\ln\left|\frac{(\mu/\hbar-\omega)^2-(\omega_0/\hbar)^2}{\omega^2-(\omega_0/\hbar)^2}\right|\right. \\ & \left.-\frac{\omega}{v_{\mathrm{F}}^2}\ln\left|\frac{(\mu/\hbar-\omega-\omega_0/\hbar)(\omega-\omega_0/\hbar)}{(\mu/\hbar-\omega+\omega_0/\hbar)(\omega+\omega_0/\hbar)}\right|\right) \\ & -\mathrm{i}\pi\frac{A_{\mathrm{c}}}{2\pi}\left(\frac{g\omega_0}{\hbar}\right)^2\left[\left(\frac{\omega}{v_{\mathrm{F}}^2}+\frac{\omega_0}{v_{\mathrm{F}}^2\hbar}\right)\theta(\omega+\omega_0/\hbar)\right. \\ & \times\theta(\mu/\hbar-\omega_0/\hbar-\omega) \\ & \left.-\left(\frac{\omega}{v_{\mathrm{F}}^2}-\frac{\omega_0}{v_{\mathrm{F}}^2\hbar}\right)\theta(\omega-\omega_0/\hbar)\theta(\mu/\hbar+\omega_0/\hbar-\omega)\right]. \end{aligned} \qquad (27)$$

We note that, for finite doping, $\Sigma_\mu^{\mathrm{ret}}(\omega)$ diverges logarithmically at $\omega = \pm\omega_0/\hbar$.

4. Optical conductivity

In this section we want to compute the optical conductivity of graphene and study how the conductivity of the system is affected by the out-of-plane (ZO)-phonons. To determine the conductivity, one needs to know the current operator j_x, which is composed of the paramagnetic and diamagnetic contributions $j_x = j_x^P + A_x(t)j_x^D$, each of them given by [33]

$$\begin{aligned} j_x^P = {} & -\frac{\mathrm{i}tea}{2\hbar}\sum_{k,\sigma}[(\phi(\boldsymbol{k})-3)a_\sigma^\dagger(\boldsymbol{k})b_\sigma(\boldsymbol{k}) \\ & -(\phi^*(\boldsymbol{k})-3)b_\sigma^\dagger(\boldsymbol{k})a_\sigma(\boldsymbol{k})], \end{aligned} \qquad (28)$$

and

$$\begin{aligned} j_x^D = {} & -\frac{te^2a^2}{4\hbar^2}\sum_{k,\sigma}[(\phi(\boldsymbol{k})+3)a_\sigma^\dagger(\boldsymbol{k})b_\sigma(\boldsymbol{k}) \\ & +(\phi^*(\boldsymbol{k})+3)b_\sigma^\dagger(\boldsymbol{k})a_\sigma(\boldsymbol{k})]. \end{aligned} \qquad (29)$$

The Kubo formula for the conductivity is given by [34]

$$\sigma_{xx}(\omega) = \frac{\langle j_x^D\rangle}{\mathrm{i}A_{\mathrm{s}}(\omega+\mathrm{i}0^+)} + \frac{\Lambda_{xx}(\omega+\mathrm{i}0^+)}{\mathrm{i}\hbar A_{\mathrm{s}}(\omega+\mathrm{i}0^+)}, \qquad (30)$$

with $A_{\mathrm{s}} = N_{\mathrm{c}}A_{\mathrm{c}}$ being the area of the sample, and A_{c} being the area of the unit cell, from which it follows that

$$\mathrm{Re}\sigma(\omega) = D\delta(\omega) + \frac{\mathrm{Im}\Lambda_{xx}(\omega+\mathrm{i}0^+)}{\hbar\omega A_{\mathrm{s}}}, \qquad (31)$$

where D is the charge stiffness, which reads

$$D = -\pi\frac{\langle j_x^D\rangle}{A_{\mathrm{s}}} - \pi\frac{\mathrm{Re}\Lambda_{xx}(\omega+\mathrm{i}0^+)}{\hbar A_{\mathrm{s}}}. \qquad (32)$$

The incoherent contribution to the conductivity $\Lambda_{xx}(\omega+\mathrm{i}0^+)$ is obtained from $\Lambda_{xx}(\mathrm{i}\omega_n)$, with this latter quantity defined as

$$\Lambda_{xx}(\mathrm{i}\omega_n) = \int_0^\beta \mathrm{d}\tau\, \mathrm{e}^{\mathrm{i}\omega_n\tau}\langle T_\tau j_x^P(\tau)j_x^P(0)\rangle. \qquad (33)$$

The relevant quantity $\mathrm{Im}\,\Lambda_{xx}(\omega+\mathrm{i}0^+)$ is given by

$$\begin{aligned} \mathrm{Im}\Lambda_{xx}(\omega+\mathrm{i}0^+) = {} & \frac{t^2e^2a^2}{16\hbar^2}\int\frac{\mathrm{d}\epsilon}{2\pi\hbar} \\ & \times\sum_{\boldsymbol{k}}\sum_{\lambda_1,\lambda_2=\pm1}[n_{\mathrm{F}}(\epsilon)-n_{\mathrm{F}}(\epsilon+\omega\hbar)] \\ & \times A^{\lambda_1}(\boldsymbol{k},\omega+\epsilon/\hbar)A^{\lambda_2}(\boldsymbol{k},\epsilon/\hbar)f(\boldsymbol{k},\lambda_1,\lambda_2), \end{aligned} \qquad (34)$$

with $A^\lambda(\boldsymbol{k},\omega)$ given by

$$A^\lambda(\boldsymbol{k},\omega) = -2\mathrm{Im}G_R^\lambda(\boldsymbol{k},\omega+\mathrm{i}0^+), \qquad (35)$$

$G^{\lambda}(\boldsymbol{k}, \mathrm{i}\omega)$ given by

$$G^{\lambda}(\boldsymbol{k}, \mathrm{i}\omega_n) = \frac{1}{\mathrm{i}\omega_n - \Sigma(\mathrm{i}\omega_n) - (\lambda t|\phi(\boldsymbol{k})| - \mu)/\hbar}, \quad (36)$$

and $f(\boldsymbol{k}, \lambda_1, \lambda_2)$ given by

$$f(\boldsymbol{k}, \lambda_1, \lambda_2) = 2|\phi(\boldsymbol{k}) - 3|^2 - \lambda_1\lambda_2\left[(\phi^*(\boldsymbol{k}) - 3)^2 \frac{\phi^2(\boldsymbol{k})}{|\phi(\boldsymbol{k})|^2} + (\phi(\boldsymbol{k}) - 3)^2 \frac{(\phi^*(\boldsymbol{k}))^2}{|\phi(\boldsymbol{k})|^2}\right]. \quad (37)$$

Using the fact that

$$\sum_{\boldsymbol{k}} \phi(\boldsymbol{k}) g(|\phi(\boldsymbol{k})|) = \sum_{\boldsymbol{k}} \phi^*(\boldsymbol{k}) g(|\phi(\boldsymbol{k})|) = \tfrac{1}{3} \sum_{\boldsymbol{k}} |\phi(\boldsymbol{k})|^2 g(|\phi(\boldsymbol{k})|), \quad (38)$$

where $g(|\phi(\boldsymbol{k})|)$ is an arbitrary function of the absolute value of $\phi(\boldsymbol{k})$, and the fact that, in the Dirac cone approximation, one has

$$\frac{\phi^2(\boldsymbol{k})}{|\phi(\boldsymbol{k})|^2} \simeq \mathrm{e}^{\mathrm{i}2\pi/3}[\cos(2\theta) - \mathrm{i}\sin(2\theta)], \quad (39)$$

and a similar expression for the complex conjugate expression $[\phi^*(\boldsymbol{k})]^2/|\phi(\boldsymbol{k})|^2$, one obtains a simplified expression for (34), given by

$$\mathrm{Im}\,\Lambda_{xx}(\omega + \mathrm{i}0^+) = \frac{t^2e^2a^2}{16\hbar^2} \times \int \frac{\mathrm{d}\epsilon}{2\pi\hbar} \sum_{\boldsymbol{k}} \sum_{\lambda_1,\lambda_2=\pm1} [n_{\mathrm{F}}(\epsilon) - n_{\mathrm{F}}(\epsilon + \omega\hbar)] \times A^{\lambda_1}(\boldsymbol{k}, \omega + \epsilon/\hbar) A^{\lambda_2}(\boldsymbol{k}, \epsilon/\hbar) \times [18 - 2|\phi(\boldsymbol{k})|^2(\lambda_1\lambda_2 + 1)]. \quad (40)$$

The expression (40) is valid only in the Dirac cone approximation, and therefore one must replace $t|\phi(\boldsymbol{k})|$ by $v_{\mathrm{F}}\hbar k$ and the integral over the momentum can be performed easily. If one ignores the effect of phonons, the calculation is straightforward, leading to a conductivity of the form (at zero doping) [33]

$$\mathrm{Re}\,\sigma(\omega) = \frac{\pi}{2}\frac{e^2}{h}\left(1 - \frac{(\hbar\omega)^2}{18t^2}\right)\tanh\left(\frac{\omega\hbar}{4k_{\mathrm{B}}T}\right). \quad (41)$$

One should note that, from equation (41), one has $\mathrm{Re}\sigma(0) = 0$ for finite T. This is not seen in figure 2, because the temperature scale is very small.

The solution of equation (40) allows us to determine the optical conductivity, taking into account the effect of Holstein phonons. In addition, we mimic the effect of impurities by adding a small imaginary part Γ to the self-energy,

$$\mathrm{Im}\,\Sigma(\omega) = \mathrm{Im}\Sigma_{\mathrm{ep}}(\omega) - \Gamma, \quad (42)$$

where $\mathrm{Im}\Sigma_{\mathrm{ep}}(\omega)$ is obtained from equation (22).

There are two types of momentum integrals in (40), which have the form

$$I_n(\epsilon/\hbar, \omega, \lambda_1, \lambda_2) = \int_0^{k_c} \mathrm{d}k \frac{k^{2n+1}}{[(A - \lambda_1 k)^2 + B^2][(C - \lambda_2 k)^2 + D^2]}, \quad (43)$$

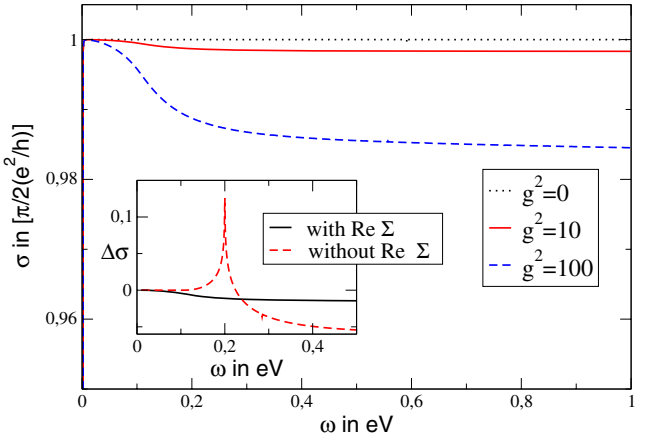

Figure 2. Optical conductivity for two different values of the coupling constant g at zero doping ($T = \Gamma = 10^{-4}$ eV). Inset: the relative conductivity $\Delta\sigma = \sigma(g = 10) - \sigma(g = 0)$ with and without $\mathrm{Re}\Sigma(\omega)$.

with $n = 0, 1$. The analytical expressions are given in the appendix. The final energy integration can be performed numerically.

In figure 2, the conductivity is shown for various coupling constants g at zero doping and low temperature T and damping Γ due to impurity scattering. There is a drop in the conductivity (relative to the conductivity of a clean system) starting at around the phonon energy ω_0 and reaching a constant value for $\omega \gtrsim 2\omega_0$. Without the real part of the electronic self-energy, there is a pronounced peak at twice the phonon energy. This is shown in the inset of figure 2, where we plot $\Delta\sigma = \sigma(g = 10) - \sigma(g = 0)$ for $T = \Gamma = 0.0001$ eV and including (respectively, not including) $\mathrm{Re}\Sigma(\omega)$ in the above expressions. It is thus crucial to include the full self-energy in the renormalization of the particle Green's function.

We thus obtain as the main result that there remains no pronounced structure in the conductivity due to ZO phonons if the full self-energy is used. We attribute this fact to the apparently asymmetric way that the self-energy enters into the Green's function with respect to the electron ($j = 1$) and hole ($j = -1$) channel, which destroys possible interference between the two carriers (see equation (22)).

In figures 3 and 4, the optical conductivity is shown for different values of the coupling constant g at $\mu = 0.05$ eV and $\mu = 0.1$ eV, respectively. The insets show the relative conductivity due to the electron–phonon interaction, $\Delta\sigma = \sigma(g = 10) - \sigma(g = 0)$, including (respectively, not including) $\mathrm{Re}\Sigma(\omega)$ in the above expressions. Again, we see a distinct difference in the result due to the renormalization of the electron–hole spectra.

It is clear that the results at finite chemical potential are markedly different from the results at the neutrality point. At finite chemical potential the system is characterized by a Drude-like behavior followed by a strong increase in the conductivity when the photon frequency reaches a value of twice the chemical potential. At zero doping there is no Drude weight and the system response is characterized only by inter-band transitions. We see only weak renormalization

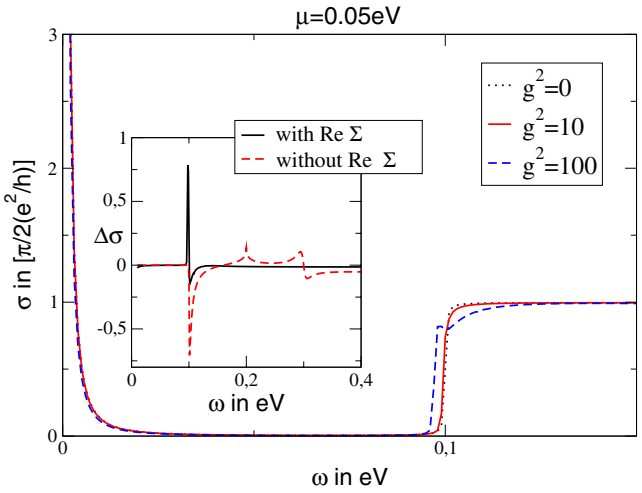

Figure 3. Optical conductivity for two different values of the coupling constant g at $\mu = 0.05$ eV ($T = \Gamma = 10^{-4}$ eV). Inset: the relative conductivity $\Delta\sigma = \sigma(g = 10) - \sigma(g = 0)$ with and without $\mathrm{Re}\,\Sigma(\omega)$.

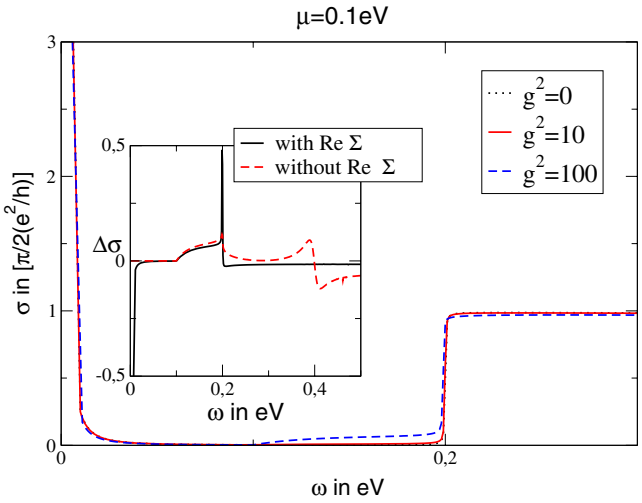

Figure 4. Optical conductivity for two different values of the coupling constant g at $\mu = 0.1$ eV ($T = \Gamma = 10^{-4}$ eV). Inset: the relative conductivity $\Delta\sigma = \sigma(g = 10) - \sigma(g = 0)$ with and without $\mathrm{Re}\,\Sigma(\omega)$.

of the Drude peak due to the Holstein phonons as well as negligible effects at finite frequencies. We note that the results for $\mathrm{Re}\,\sigma(\omega)$ when $g = 0$ were first obtained by Peres *et al* [24] and by Gusynin *et al* [35].

5. Summary

In this paper, we have calculated the effect of Holstein polarons on the electronic properties of graphene. Holstein polarons arise through the coupling of out-of-plane optical (ZO) modes to the conduction electrons, described as Dirac fermions. Throughout this work, we assumed Migdal's theorem to be valid and calculated the electronic self-energy within the first Born approximation. We find that the Fermi velocity becomes renormalized within 1%.

The main purpose of this work was to assess the effect of Holstein phonons on the conductivity within the Kubo formula. Due to the large phonon energy, electron scattering from Holstein phonons induces inter-band transitions for the usual carrier densities (corresponding to a gate voltage of ∼50 V) and can thus not be treated within the one-band Boltzmann approach. We thus calculated the optical conductivity within the Kubo formula, employing the full Green's function but neglecting vertex corrections. We find a pronounced kink-like peak at twice the ZO phonon energy if only the imaginary part of the self-energy is considered. This peak vanishes when the real part of the self-energy is included. Further, we see only weak renormalization of the Drude peak due to the Holstein phonons as well as negligible effects at finite frequencies. We conclude that scattering from Holstein phonons can be neglected in the usual transport properties.

The effect of lattice vibrations on the electronic properties of graphene is still not fully understood. The coupling of substrate phonons [36] or in-plane oscillations to the conduction electrons is especially interesting. In the later case, this will lead to a non-diagonal electronic self-energy due to the current–current coupling.

Acknowledgments

The authors want to thank F Guinea and A H Castro Neto for useful discussions. This work has been supported by the Ministrio de Educación y Ciencia (Spain) through grant no. FIS2004-06490-C03-01, the Juan de la Cierva Programme, and by the European Union through contract 12881 (NEST). N M R Peres thanks the European Science Foundation Programme INSTANS 2005-2010, and the Fundação para a Ciência e a Tecnologia under the grant PTDC/FIS/64404/2006.

Appendix. Momentum integrals

The momentum integrals have the form ($n = 0, 1$)

$$I_n = \int \frac{k^{2n+1}\mathrm{d}k}{[(A-k)^2 + B^2][(C-k)^2 + D^2]}. \tag{A.1}$$

The general solution yields

$$I_n = \frac{-1}{G}\left[F_1^n \tan^{-1}\left(\frac{A-k}{B}\right) + F_2^n \tan^{-1}\left(\frac{C-k}{D}\right) - F_3^n \ln\left((A-k)^2 + B^2\right) - F_4^n \ln\left((C-k)^2 + D^2\right)\right], \tag{A.2}$$

where the denominator reads $G = (B^2 + (A-C)^2)^2 + 2((A-C)^2 - B^2)D^2 + D^4$ and the factors are given by

$$F_1^0 = 4D(A^3 - 2A^2C - 2B^2C + A(B^2 + C^2 + D^2)),$$

$$F_2^0 = 4B((B^2 + (A-C)^2)C + (-2A + C)D^2),$$

$$F_3^0 = -F_4^0 = 2BD(-A^2 - B^2 + C^2 + D^2)$$

and

$$F_1^1 = 4D(A^5 - 2A^4C + 2B^4C + A^3(2B^2 + C^2 + D^2) + AB^2(B^2 - 3(C^2 + D^2))),$$
$$F_2^1 = 4B((B^2 + (A - C)^2)C^3 + C(-3(A^2 + B^2) + 2C^2)D^2 + (2A + C)D^4),$$
$$F_3^1 = 2BD(A^4 - 4A^3C - 4AB^2C + B^2(B^2 - C^2 - D^2) + A^2(2B^2 + 3(C^2 + D^2))),$$
$$F_4^1 = 2BD(C^2(3(A^2 + B^2) - 4AC + C^2) - (A^2 + B^2 + 4AC - 2C^2)D^2 + D^4).$$

References

[1] Novoselov K S, Geim A K, Morozov S V, Jiang D, Zhang Y, Dubonos S V, Grigorieva I V and Firsov A A 2004 *Science* **306** 666
[2] Geim A K and Novoselov K S 2007 *Nat. Mater.* **6** 183
[3] Stein G E, Kramer E J, Li X and Wang J 2007 *Phys. Rev. Lett.* **98** 086101
[4] Meyer J C, Geim A K, Katsnelson M I, Novoselov K S, Booth T J and Roth S 2007 *Nature* **446** 60
[5] Xiaoguang W, Peeters F M and Devreese J T 1985 *Phys. Rev.* B **31** 3420
Das Sarma S and Mason B A 1985 *Ann. Phys.* **163** 78
[6] Sood A K, Menéndez J, Cardona M and Ploog K 1985 *Phys. Rev. Lett.* **54** 2111
Trallero-Giner C, García-Moliner F, Velasco V R and Cardona M 1992 *Phys. Rev.* B **45** 11944
Shields A J, Cardona M and Eberl K 1994 *Phys. Rev. Lett.* **72** 412
[7] Su W P, Schrieffer J R and Heeger A J 1979 *Phys. Rev. Lett.* **42** 1698
[8] Mañes J L 2007 *Phys. Rev.* B **76** 045430
[9] Holstein T 1959 *Ann. Phys.* **8** 325
Holstein T 1959 *Ann. Phys.* **8** 343
[10] Goodvin G L, Berciu M and Sawatzky G A 2006 *Phys. Rev.* B **74** 245104
[11] Falkovsky L A 2007 *Preprint* cond-mat/0702409
[12] Wirtz L and Rubio A 2004 *Solid State Commun.* **131** 141
[13] Sasaki K, Sato K, Jiang J, Saito R, Onari S and Tanaka Y 2007 *Phys. Rev.* B **75** 235430
[14] Castro Neto A H and Guinea F 2007 *Phys. Rev.* B **75** 045404
[15] Alvermann A, Edwards D M and Fehske H 2007 *Phys. Rev. Lett.* **98** 056602
[16] Nomura K and MacDonald A H 2006 *Phys. Rev. Lett.* **96** 256602
[17] Adam S, Hwang E H, Galitski V M and Das Sarma S 2007 *Proc. Natl Acad. Sci. USA* **104** 18392
[18] Peres N M R, Lopes dos Santos J M B and Stauber T 2007 *Phys. Rev.* B **76** 073412
[19] Stauber T, Peres N M R and Guinea F 2007 *Phys. Rev.* B **76** 205423
[20] Hwang E H, Adam S, Das Sarma S and Geim A K 2007 *Phys. Rev.* B **76** 195421
[21] Auslender M and Katsnelson M I 2007 *Preprint* 0707.2804
[22] Lazzeri M and Mauri F 2006 *Phys. Rev. Lett* **97** 266407
[23] Fröhlich H 1954 *Adv. Phys.* **3** 325
[24] Peres N M R, Guinea F and Castro Neto A H 2006 *Phys. Rev.* B **73** 125411
[25] Mahan G D 2000 *Many-Particle Physics* 3rd edn (New York: Kluwer/Plenum)
[26] Migdal A B 1958 *Zh. Eksp. Teor. Fiz.* **34** 1438
Migdal A B 1958 *Sov. Phys.—JETP* **7** 996 (Engl. Transl.)
[27] Schmitt-Rink S, Miller D A B and Chemla D S 1987 *Phys. Rev.* B **35** 8113
[28] Stauber T and Zimmermann R 2006 *Phys. Rev.* B **73** 115303
[29] Gunnarsson O, Meden V and Schönhammer K 1994 *Phys. Rev.* B **50** 10462
[30] Meden V, Schönhammer K and Gunnarsson O 1994 *Phys. Rev.* B **50** 11179
[31] Aleiner I L and Efetov K B 2006 *Phys. Rev. Lett.* **97** 236801
[32] Stauber T, Guinea F and Vozmediano M A H 2005 *Phys. Rev.* B **71** 041406(R)
[33] Peres N M R and Stauber T 2008 *Int. J. Mod. Phys.* B at press
[34] Paul I and Kotliar G 2003 *Phys. Rev.* B **67** 115131
[35] Gusynin V P, Sharapov S G and Carbotte J P 2006 *Phys. Rev. Lett.* **96** 256802
[36] Fratini S and Guinea F 2007 *Preprint* 0711.1303 (unpublished)